Angewandte Communications

Gas-Phase Chemistry

DOI: 10.1002/anie.201((will be filled in by the editorial staff))

Gas Phase Synthesis of the Benzyl Radical ($C_6H_5CH_2$)**

Beni B. Dangi, Dorian S. N. Parker, Tao Yang, Ralf I. Kaiser, Alexander M. Mebel**

Abstract: Dicarbon (C_2) represents the simplest bare carbon molecule, which is ubiquitous in the interstellar medium and in combustion flames. Here, we report on a novel gas phase synthesis of the benzyl radical ($C_6H_5CH_2$) via the crossed molecular beam reaction of dicarbon, $C_2(X^1\Sigma_g^+, a^3\Pi_u)$, with 2-methyl-1,3-butadiene (isoprene; C_5H_8; X^1A') accessing the triplet and singlet C_7H_8 potential energy surfaces (PESs) under single collision conditions. The experimental data were combined with ab initio and statistical calculations to reveal the underlying reaction mechanism and chemical dynamics. On the singlet and triplet surfaces, the reactions involve indirect scattering dynamics and are initiated by the barrier-less addition of dicarbon to the carbon–carbon double bond of the 2-methyl-1,3-butadiene molecule. These initial addition complexes rearrange via multiple isomerization steps involving cyclization and hydrogen shifts leading eventually to the formation of C_7H_7 radical species through atomic hydrogen elimination. The benzyl radical ($C_6H_5CH_2$), which presents the thermodynamically most stable C_7H_7 isomer, is determined to be the major product. This reaction demonstrates *the synthesis of the prototype of an aromatic (AR) and resonantly stabilized free radical (RSFR)* - the benzyl radical - via a previously unknown reaction route involving a single collision. From synthetic point of view, the formation of a cyclic product from two acyclic reactants - dicarbon and isoprene - presents a benchmark system, which opens up future investigations on this reaction class leading to (substituted) phenyl and benzyl-type radicals via a single collision event in the gas phase.

[*] Dr. B. B. Dangi, Dr. D. S. N. Parker, Dr. T. Yang, Prof. R. I. Kaiser

Department of Chemistry

University of Hawai'i at Manoa

Honolulu, HI 96822 (USA)

Fax: (+1) 808-956-5908

E-mail: ralfk@hawaii.edu

Homepage: http:// www.chem.hawaii.edu/Bil301/welcome.html

Prof. A. M. Mebel

Department of Chemistry and Biochemistry

Florida International University

Miami, FL 33199 (USA)

[**] This work was supported by the US Department of Energy, Basic Energy Sciences, via grants DE-FG02-03ER15411 (Hawaii) and DE-FG02-04ER15570 (Florida).

Supporting information for this article is available on the WWW under http://dx.doi.org/10.1002/anie.201xxxxxx.((Please delete if not appropriate))

Astrochemical and combustion models on the formation of polycyclic aromatic hydrocarbon (PAH) propose molecular weight growth processes through sequential reactions of aromatic (AR) and resonantly stabilized free radicals (RSFR) eventually leading to carbonaceous nanoparticles.[1-2] Along with acetylene, these pathways are considered as the basis for the hydrogen abstraction-acetylene addition (HACA),[3] phenyl addition-cyclization (PAC),[4] ethynyl addition (EA),[5] and vinylacetylene addition (VA)[6] mechanisms. Due to their stability even at elevated temperatures of several thousand Kelvin, RSFRs and ARs can reach high concentrations in flames and in extraterrestrial environments such as in circumstellar envelopes of carbon stars. These high concentrations make them important reaction intermediates to be involved in mass growth processes and hence in the formations of PAHs. During the last decade, particular focus has been directed to the role of the C_7H_7 radicals including benzyl ($C_6H_5CH_2$), o-, m-, and p-tolyl (2-, 3-, and 4-tolyl) ($C_6H_4CH_3$), and cycloheptatrienyl (C_7H_7) radicals (Scheme 1).[7-9] Here, benzyl ($C_6H_5CH_2$) has been proposed to yield indene (C_9H_8) upon reaction with acetylene (C_2H_2).[10],[11] Indene may further produce indenyl radical(s). These indenyl radical(s) may then react with vinylacetylene (C_4H_4) to lead to fluorene, 1H-benz[f]indene, 1H-benz[e]indene, and/or 1H-phenalene. Due to the potential key role of the benzyl ($C_6H_5CH_2$) radical, which is both aromatic and resonantly stabilized, in the formation of PAHs carrying five membered rings, reaction mechanisms to distinct C_7H_7 isomers involving the phenyl radical (C_6H_5), fulvenallene (C_7H_6), 1-ethynyl-cyclopentadiene (C_7H_6), and the propargyl radical (C_3H_3) have been explored computationally.[7-8, 12-13] However, the formation of C_7H_7 isomers - among them the thermodynamically most stable benzyl ($C_6H_5CH_2$) radical – via the bimolecular reaction of ubiquitous dicarbon molecules (C_2) with C_5H_8 isomers such as 2-methyl-1,3-butadiene (isoprene, C_5H_8; X^1A') has never been contemplated. The dicarbon molecule is abundant in hydrocarbon flames and in the interstellar medium while the 2-methyl-1,3-butadiene can be formally derived from 1,3-butadiene (C_4H_6) by replacing the hydrogen atom at the C2 carbon atom by a methyl group. The 1,3-butadiene together with its C_4H_6 isomers 1,2-butadiene, 1-butyne, and 2-butyne is omnipresent in combustion flames such as of ethylene and cyclohexane. Further, C_5H_8 isomers have been probed in hydrocarbon flames, where the benzyl ($C_6H_5CH_2$) radical is determined as the major C_7H_7 species. Because of its resonant *and* aromatic stabilization, benzyl reaches significant concentrations in combustion flames and hence an understanding of its chemistry, in particular its formation and decomposition processes as well as bimolecular reactions, is essential for the development of accurate and predictive combustion engine models. Here, we report the results of crossed molecular beams reaction of dicarbon with 2-methyl-1,3-butadiene accessing various chemically activated reactive intermediates on the singlet and triplet C_7H_8 surfaces, which then decompose to products including distinct C_7H_7 isomers. These systems are also interesting from the viewpoint of a physical–organic chemist as they represent benchmarks to unravel the chemical reactivity, bond breaking processes, and the synthesis of truly combustion and astrochemically relevant cyclic and aromatic hydrocarbon radicals from acyclic precursors via bimolecular gas phase reactions in single collision events.

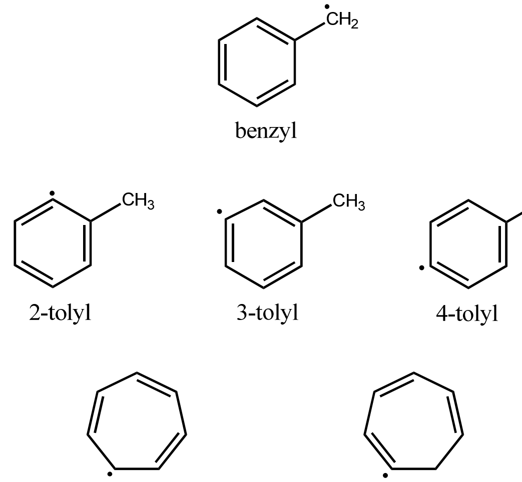

Scheme 1. Structures of the most common C_7H_7 radicals.

Reactive scattering signal from the reactions of dicarbon (C_2; 24 amu) with 2-methyl-1,3-butadiene (C_5H_8; 68 amu) was observed at m/z = 91 ($C_7H_7^+$), m/z = 90 ($C_7H_6^+$) and m/z = 89 ($C_7H_5^+$) with data at m/z = 89 depicting the best signal-to-noise. The time-of-flight (TOF) spectra at these mass-to-charge rations were - after scaling – superimposable, suggesting that signal at m/z = 90 and 89 originated from dissociative ionization of the C_7H_7 product in the electron impact ionizer of the detector; here, if TOF data at two mass-to-charge ratios (m/z) are overlapping, data at lower m/z are fragments from higher m/z. Therefore, our data suggest that only the dicarbon versus atomic hydrogen exchange channel is open, and that the molecular hydrogen loss pathways are closed. We would like to emphasize that in addition to dicarbon, the primary beam also contains atomic carbon and tricarbon molecules; however, tricarbon is unreactive with isoprene and hence does not interfere with the scattering signal obtained at lower mas-to-charge ratios. This is evident from the lack of any reactive scattering signal at m/z = 103 ($C_8H_7^+$), 102 ($C_8H_6^+$), and 101 ($C_8H_5^+$). Further, signal at m/z = 91, 90, and 89 cannot be fit with a reactant mass combination of 36 amu (tricarbon) plus 68 amu (isoprene); therefore, this signal does not originate from dissociative ionization of any reactively scattered products in the tricarbon - C_5H_8 system. Likewise, ground state carbon atoms would react with the C_5H_8 isomer to products with molecular masses of 79 amu and less; therefore, reactions of carbon does not contribute to scattering signal at m/z = 91 to 89. Figure 1 presents selected TOF spectra recorded at various angles in the laboratory frame for the most intense fragment ion m/z = 89 ($C_7H_5^+$). These TOF spectra can be integrated to derive the laboratory angular distribution of the C_7H_7 product(s); this distribution peaks close to the center-of-mass (CM) angle of 44.1±1.3^0 and depicts a nearly forward-backward symmetric distribution extending at least 40^0 with the scattering plane defined by both beams. These patterns indicate indirect scattering dynamics through the formation of C_7H_8 reaction intermediates on the singlet and triplet surfaces. In summary, the interpretation of the TOF data alone suggests the existence of dicarbon versus hydrogen atom exchange channel(s) and the formation of C_7H_7 isomer(s).

First, we would like to interpret the experimental data and present the information, which can be obtained from the crossed molecular beam experiments. For this, the laboratory data are converted into the center-of-mass (CM) reference frame to obtain the translational energy ($P(E_T)$) and angular ($T(\theta)$) distributions as shown in Figure 2. The $P(E_T)$ peaks slightly away from zero translational energy at around 20-30 kJ mol^{-1} suggesting that at least one channel holds a tight exit transition state upon decomposition of the C_7H_8 intermediate(s);[14] this process is connected with a significant electron rearrangement upon the formation of the C_7H_7 product. Further, the maximum of the translational energy of the $P(E_T)$ resembles the sum of the collision energy plus the reaction energy for those product molecules without internal excitation. Therefore, the maximum translational energy releases can be utilized to extract the reaction energy and hence, upon comparison with computed reaction energies, also the structural isomer formed. Considering the maximum translational energy of 525 ± 30 kJ mol^{-1}, the reaction is determined to be exoergic by 482 ± 32 kJ mol^{-1} after subtracting the nominal collision energies (Supporting information). Recall that the dicarbon beam also holds molecules in its first electronically excited state $a^3\Pi_u$, which lies higher by 8 kJ mol^{-1} compared to its $X^1\Sigma_g^+$ ground state.[15] Therefore, a subtraction of this energy indicates that the reaction of dicarbon with 2-methyl-1,3-butadiene is exoergic by 474 ± 32 kJ mol^{-1}. Finally, the translational energy distribution helps to calculate the averaged fraction of available energy released into the translational degrees of freedom to be 26 ± 5%; this order of magnitude proposes indirect reaction dynamics.[16] The $T(\theta)$ distribution is forward-backward symmetric with respect to 90^0 and is distributed over the complete angular range of 0^0 to 180^0. This finding suggests that this reaction follows indirect scattering dynamics via the formation of C_7H_8 reaction intermediate(s). Also, the distribution maximum of the center-of-mass angular distribution at 90^0 indicates 'sideways scattering', i.e. the departing atomic hydrogen atom is emitted preferentially perpendicularly with respect to the rotational plane of the decomposing complex.[17] This finding is also reflected in the flux contour map as depicted in the table of contents graphic.

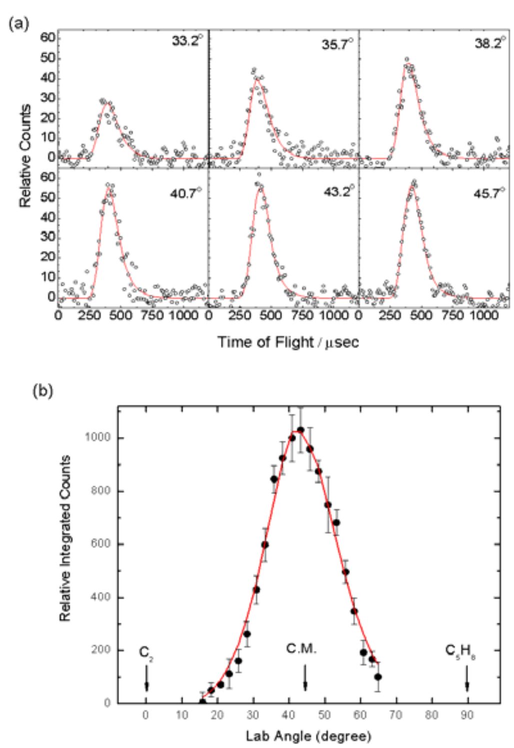

Figure 1. Time-of-flight data (a) and laboratory angular distribution (b) at m/z = 89 ($C_7H_5^+$) for the reaction of dicarbon (C_2) with isoprene (C_5H_8) forming C_7H_7 product(s) at collision energy of 42.7 ± 1.5 kJ mol^{-1}. The circles represent the experimental data, error bars present the standard deviation and the solid lines represent the fit.

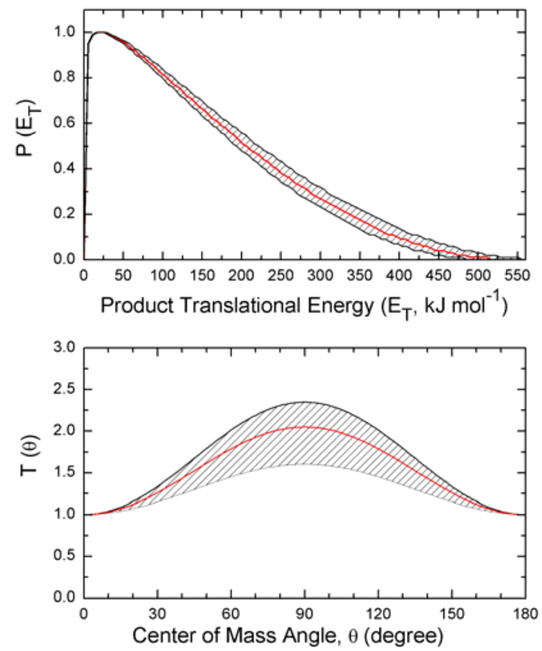

Figure 2. Center-of-mass translational energy flux distribution (upper) and angular distribution (lower) for the hydrogen atom loss channel in the reaction of dicarbon with isoprene leading to C_7H_7 product(s). Hatched areas indicate the acceptable upper and lower error limits of the fits and solid red lines define the best-fit functions.

Second, we also explored the reaction of singlet and triplet dicarbon with isoprene computationally; the singlet and triplet C_7H_8 potential energy surfaces (PESs) are presented in Figures 3 and 4. Considering the singlet surface, dicarbon can add without entrance barrier to either the C3-C4 or the C1-C2 carbon-carbon double bonds of isoprene yielding intermediates **si1** and **si2**, respectively. These collision complexes ring open to **si3** and **si4**, respectively. Both acyclic intermediates may undergo hydrogen shifts yielding eventually intermediate **si5**, which then undergoes a trans-cis conversion to **si6** through a low barrier of only 21 kJ mol^{-1}. A hydrogen shift in the latter yields **si7**, which subsequently isomerizes via cis-trans conversion to **si8**. This intermediate can undergo ring closure to **si9** or **si10**, the ring closure to the former is initiated with a 1,3-H atom shift from the methyl group. Considering the inherent barriers of 340 and 145 kJ mol^{-1}, the formation of **si10** should be preferential. This species depicts a hydrogen shift at the ring from the para to the meta position to **si11**, with the latter isomerizing via yet another hydrogen migration to **si12** (toluene). Toluene represents the global minimum on the C_7H_8 potential energy surface and can undergo unimolecular decomposition involving atomic hydrogen loss via four simple bond rupture processes. These form the benzyl radical ($C_6H_5CH_2$) and/or o-, m-, and/or p-tolyl radicals. The benzyl radical is thermodynamically more stable by about 94 kJ mol^{-1} compared to the tolyl radicals due to resonance stabilization of the radical center. Note that **si1** and **si2** can also react to products other than C_7H_7 (Supporting information Figure S1).

Figure 4 shows the reaction paths for addition of triplet dicarbon to the isoprene. The triplet dicarbon can add without entrance barrier to the C4 and C1 carbon atoms of isoprene yielding intermediates **ti1** and **ti2**, respectively, which are bound by 180 and 190 kJ mol^{-1} with respect to the separated reactants. These intermediates isomerize via hydrogen shifts and ring closures involving **ti3**, **ti6**, **ti11**, **ti12**, and **ti13** to eventually form the cyclic structures **ti4**, **ti7**, **ti8**, and **ti10**. Considering the inherent barriers to isomerization, all isomerization pathways involving **ti3** and **ti12** yield **ti4**, with **ti7** leading to **ti10** and **ti8**. What is the fate of these cyclic intermediates? Intermediate **ti4** isomerizes via hydrogen shift to **ti5**, which then decomposes to the benzyl radical through a tight exit transition state located 16 kJmol^{-1} above the separated products. **ti8** and **ti10** preferentially decompose by atomic hydrogen losses yielding m- and p-tolyl radicals, respectively, or undergo distinct hydrogen shifts (via **ti9**) and then dissociate to the benzyl radical ($C_6H_5CH_2$) and/or o-, m-, and/or p-tolyl radicals, or phenyl plus the methyl radical (CH_3). Note that with the exception of the decomposition of **ti9** to the benzyl radical, all exit transition states are tight. Intermediates **ti1** and **ti2** can also decompose to acyclic products (Supporting information Figures S1, however, these pathways are energetically not favorable.

Having interpreted the experimental data and the potential energy surfaces, we are merging now the experimental findings (reaction energies, exit barriers, indirect nature of the reaction mechanism, and geometry of the exit transition state) with the computational data. A comparison of the experimentally determined exoergicity of the reaction of dicarbon with 2-methyl-1,3-butadiene of 474 ± 32 kJ mol^{-1} with the computed reaction energies (477 ± 10 kJ) suggests the formation of at least the thermodynamically most stable C_7H_7 isomer: the benzyl radical (C_6H_5 CH_2). Considering that the experimentally determined off-zero peaking at 20 to 30 kJ mol^{-1} of the center-of-mass translational energy distribution suggests a tight exit transition state, the computational data propose that at least one decomposition pathway involves **ti5**. Here, **ti5** undergoes hydrogen loss via a barrier located 16 kJmol^{-1} above the separated products; the unimolecular decomposition of **ti9** is barrier-less and hence not expected to result in an off-zero peaking of the center-of-mass translational energy distribution. How can **ti5** be formed? Considering the triplet surface, **ti5** is most likely reached from **ti1** via **ti3** and **ti4** or from **ti2** via **ti11**, **ti12**, and **ti4** involving hydrogen migrations and cyclization. Based on these considerations, we can conclude that on the triplet surface, triplet dicarbon adds to the C4 or C1 carbon atom of 2-methyl-1,3-butadiene yielding intermediates **ti1** and **ti2**, respectively. Intermediate **ti1** undergoes hydrogen migration to form **ti3**, which then ring closures to **ti4**. Alternatively, **ti2** features a hydrogen shift to **ti11** followed by rotation around a C-C bond (to **ti12**) and a ring closure to **ti4**. This intermediate undergoes yet another hydrogen migration to **ti5**, which ultimately eliminates atomic hydrogen to form the benzyl radical. These indirect scattering dynamics were also predicted based on the center-of-mass angular distribution. Finally, recall that based on the center-of-mass angular distribution, the exit transition state was suggested to hold geometrical constraints depicting a hydrogen atom loss almost perpendicularly to the rotating plane of the decomposing complex. This finding was also confirmed computationally predicting an angle of the hydrogen elimination of 81.3^0 (Figure 5). Note that based on the experimentally derived energetics alone, we cannot rule out the formation of thermodynamically less stable C_7H_7 radicals. Our statistical RRKM calculations predict that upon dicarbon addition to C1 under our experimental conditions, the benzyl radical dominates and is formed at fractions of about 61% with tolyl radicals contributing to about 37% with nearly equal contributions of m- and p-tolyl; further, non-aromatic products are minor and contribute only 2%. Adding dicarbon to C4 produces about 25% benzyl and 75% m- and p-tolyl. The higher yield of benzyl computed for the C1 addition is determined by the fact that the barrier for the **ti2** → **ti11** isomerization eventually leading to **ti4** is 20 kJ mol^{-1} lower than that for the competing **ti2** → **ti13** process, whereas the barriers for **ti1** → **ti3** on the path to **ti4** and **ti1** → **ti6** are nearly equal. If the C1 and C4 additions are equally split, we expect about 43% of benzyl.

The computations predict further that on the singlet surface, the addition to the C3-C4 and C1-C2 may yield – via the collision complexes **si1** and **si2** - eventually **si8** via a multi-step isomerization sequence involving successive hydrogen shifts. Considering the barrier to isomerization, intermediate **si8** is expected to rearrange to **si10**, which eventually yields singlet toluene (**si12**). The latter is expected to decompose via lose exit transition states to the benzyl as well as tolyl radicals with benzyl being formed preferentially. However, before intermediate **si8** can be even formed, the reaction can alternatively proceed by numerous fragmentation channels involving H, CH_3, and C_3H_3 elimination and the production of non-aromatic radicals (Supporting information Figure S1). We conclude therefore that the addition of singlet dicarbon to the C3-C4 bond of 2-methyl-1,3-butadiene most likely forms non-aromatic $CH_2CCCHCCH_2$ plus methyl and **sp2-sp4** plus atomic hydrogen and the pathway from **si3** to the aromatic products is effectively closed. For **si4**, the barrier for the H shift to form **si5** is 292 kJ mol^{-1}, 46 and 54 kJ mol^{-1} lower than the energies required for the CH_3 loss leading to $CH_2CHCCCCH_2$ and for the hydrogen loss producing **sp11**. Hence, the channel from **si4** to **si5** and then to **si8** and to benzyl can be in principle competitive. Nevertheless, we do not expect a high yield of benzyl from the singlet C_2 addition to the C1-C2 bond of 2-methyl-1,3-butadiene either. Our consideration is based on the comparison with the reaction of dicarbon with 1,3-butadiene earlier studied by us.[18] Computationally, the RRKM computed branching ratios were 44% for non-aromatic C_6H_5 radicals from the intermediate analogous to **si4**, 35% for propargyl plus propargyl (from the intermediate analogous to **si5**), and only 21% for the phenyl radical. The PES calculated for dicarbon plus 2-methyl-1,3-butadiene, from **si2** to **si4** and eventually to **si12**, is similar to that for dicarbon plus 1,3-butadiene, with methyl being merely a spectator group until **si12** is formed. Moreover, while the relative energy of the **si4-si5** transition state, which represents the bottleneck on the pathway to the aromatic products, is similar to that for its analogue in the dicarbon – 1,3-butadiene reaction, the most favorable non-aromatic fragmentation products of **si4** reside 35-50 kJ mol^{-1} lower in energy than their counterparts in the dicarbon – 1,3-butadiene system and therefore the fragmentation processes of **si4** competing with its isomerization to **si5** should be relatively faster than for its analogue. In addition, **si4** can isomerize to **si15** via a barrier 7 kJ mol^{-1} lower than that for **si4** → **si5** and **si15** can decompose to CH_2CHCCH_2 plus C_3H_3 or **sp11** plus atomic hydrogen further reducing the reaction flow to **si5** and eventually to **si12**. Hence, we can suggest that the yield of benzyl radical from dicarbon addition to the C1-C2 bond of 2-methyl-1,3-butadiene should be less than 21%.

In summary, by merging the experimental and computational data, we provided compelling evidence that on the triplet surface the thermodynamically most stable a*romatic and resonantly stabilized free radical benzyl* is formed preferentially. This reaction provides a barrier-less and hitherto overlooked reaction pathway via a single collision event from acyclic, non-aromatic reactants. Since the reaction has no entrance barrier, is exoergic, and all transition states involved are located below the energy of the separated reactants, the reaction of triplet dicarbon with isoprene may form benzyl radical not only in high temperature combustion flames, but also in low temperature astrochemical environments. On the other hand, on the singlet surface, the benzyl radical is expected to be of minor importance. Further, the replacement of a hydrogen atom by a methyl group in the 1,3-butadiene reactant leads to an active participation of the methyl group in the reaction dynamics to form the benzyl radical and not just purely a spectator. Therefore, reactions of simple C1 to C3 combustion relevant radicals are expected to follow a unique chemistry once reacting with methyl- and even alkyl-substituted reactants, which is anticipated to be remarkably distinct from their non-alkyl substituted counterparts.

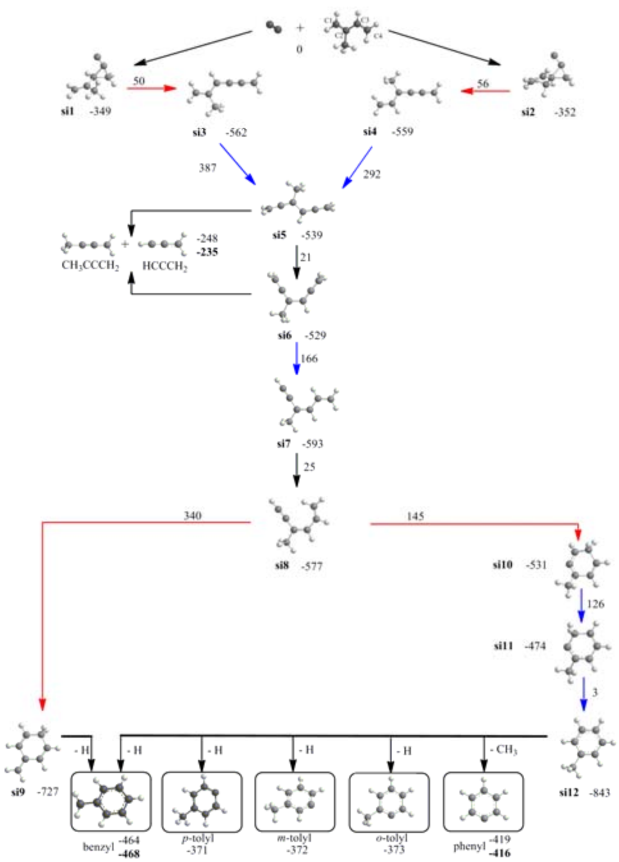

Figure 3. Low energy paths for the reaction of singlet dicarbon with isoprene leading to benzyl and tolyl products. Intermediates are labeled as **si** along with the energies relative to separated reactants and barrier heights, where applicable, in kJ mol^{-1} as calculated at the CCSD(T)/CBS(dt)//B3LYP/6-311G**+ZPE (B3LYP/6-311G**) (plain numbers) and CCSD(T)/CBS(dtq)//B3LYP/6-311G**+ ZPE(B3LYP/6-311G**) (bold numbers) levels of theory. Hydrogen shifts and isomerization via ring closure/opening are presented via blue and red arrows, respectively. For clarification, the carbon atoms in isoprene are labeled as C1 to C4.

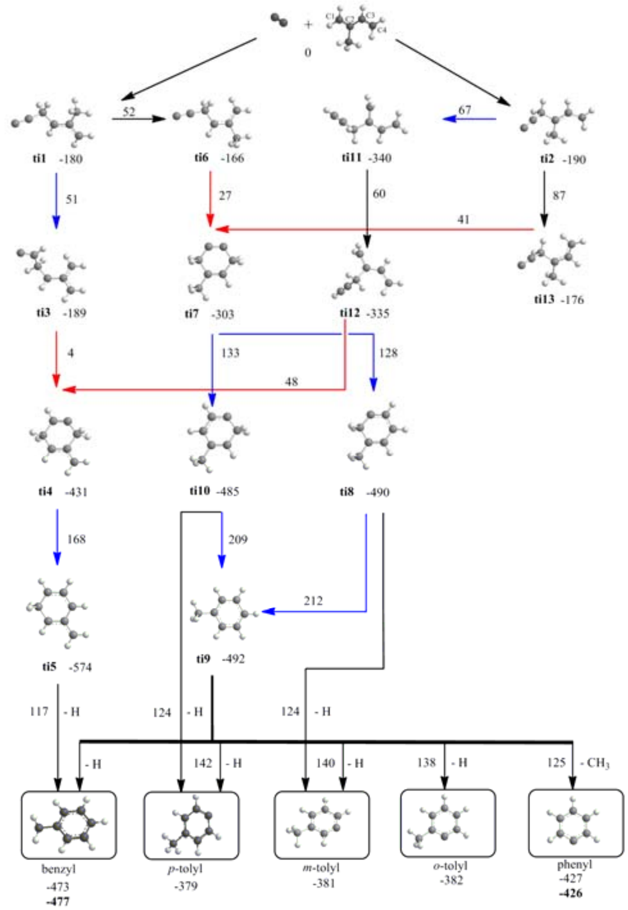

Figure 4. Low energy paths for the reaction of triplet dicarbon with isoprene leading to benzyl and tolyl products. Intermediates are labeled as **ti** along with the energies relative to separated reactants and barrier heights, where applicable, in kJ mol^{-1} as calculated at the CCSD(T)/CBS(dt)//B3LYP/6-311G**+ZPE (B3LYP/6-311G**) (plain numbers) and CCSD(T)/CBS(dtq)//B3LYP/6-311G**+ ZPE(B3LYP/6-311G**) (bold numbers) levels of theory. Hydrogen shifts and isomerization via ring closure/opening are presented via blue and red arrows, respectively. For clarification, the carbon atoms in isoprene are labeled as C1 to C4.

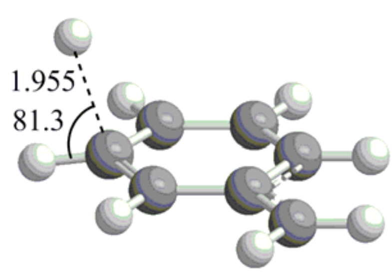

Figure 5. Computed geometry of the exit transition state from intermediate **ti5** leading to the formation of benzyl radical.

Received: ((will be filled in by the editorial staff))
Published online on ((will be filled in by the editorial staff))

Keywords: benzyl radical • bimolecular reaction • combustion chemistry • gas phase chemistry • reaction dynamics

[1] Z. A. Mansurov, *Combust. Explo. Shock+* **2005**, *41*, 727.
[2] I. Cherchneff, *Astron. Astrophys.* **2012**, *545*.
[3] H. Bockhorn, F. Fetting, A. Heddrich, G. Wannemacher, *Ber. Bunsen. Phys. Chem.* **1987**, *91*, 819.
[4] M. Shukla, A. Susa, A. Miyoshi, M. Koshi, *J. Phys. Chem. A* **2008**, *112*, 2362.
[5] A. M. Mebel, V. V. Kislov, R. I. Kaiser, *J. Am. Chem. Soc.* **2008**, *130*, 13618.
[6] D. S. N. Parker, F. T. Zhang, Y. S. Kim, R. I. Kaiser, A. Landera, V. V. Kislov, A. M. Mebel, A. G. G. M. Tielens, *P. Natl. Acad. Sci. USA* **2012**, *109*, 53.
[7] G. da Silva, J. A. Cole, J. W. Bozzelli, *J. Phys. Chem. A* **2010**, *114*, 2275.
[8] M. Derudi, D. Polino, C. Cavallotti, *Phys. Chem. Chem. Phys.* **2011**, *13*, 21308.
[9] T. C. Zhang, L. D. Zhang, X. Hong, K. W. Zhang, F. Qi, C. K. Law, T. H. Ye, P. H. Zhao, Y. L. Chen, *Combust. Flame* **2009**, *156*, 2071.
[10] L. Vereecken, J. Peeters, *Phys. Chem. Chem. Phys.* **2003**, *5*, 2807.
[11] W. M. Davis, S. M. Heck, H. O. Pritchard, *J. Chem. Soc. Faraday T.* **1998**, *94*, 2725.
[12] S. J. Klippenstein, L. B. Harding, Y. Georgievskii, *P. Combust. Inst.* **2007**, *31*, 221.
[13] V. V. Kislov, A. M. Mebel, *J. Phys. Chem. A* **2007**, *111*, 3922.
[14] S. A. Safron, N. D. Weinstein, D. R. Herschbach, J. C. Tully, *Chem. Phys. Lett.* **1972**, *12*, 564.
[15] R. I. Kaiser, P. Maksyutenko, C. Ennis, F. T. Zhang, X. B. Gu, S. P. Krishtal, A. M. Mebel, O. Kostko, M. Ahmed, *Faraday Discuss.* **2010**, *147*, 429.
[16] R. D. Levine, *Molecular Reaction Dynamics*, Cambridge University Press, Cambridge, UK, **2005**.
[17] W. B. Miller, S. A. Safron, D. R. Herschbach, *Discuss. Faraday Soc.* **1967**, *44*, 108.
[18] F. T. Zhang, B. Jones, P. Maksyutenko, R. I. Kaiser, C. Chin, V. V. Kislov, A. M. Mebel, *J. Am. Chem. Soc.* **2010**, *132*, 2672.

Entry for the Table of Contents (Please choose one layout)

Layout 1:

Reaction Dynamics

*Beni B. Dangi, Dorian S. N. Parker, Tao Yang, Ralf I. Kaiser, * Alexander M. Mebel**

__________ **Page – Page**

A Combined Experimental and Theoretical Study on the Gas Phase Synthesis of the Benzyl Radical ($C_6H_5CH_2$) under Single Collision Conditions

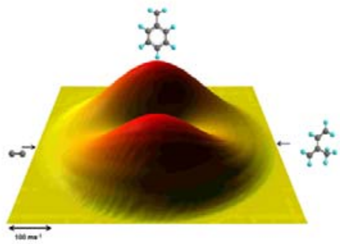

Crossed molecular beam experiments and ab initio electronic structure calculations on the reaction of dicarbon with isoprene are presented. The picture shows a flux contour map of the reaction of dicarbon with isoprene forming benzyl radical and atomic hydrogen at a collision energy of 43 kJ mol^{-1}.

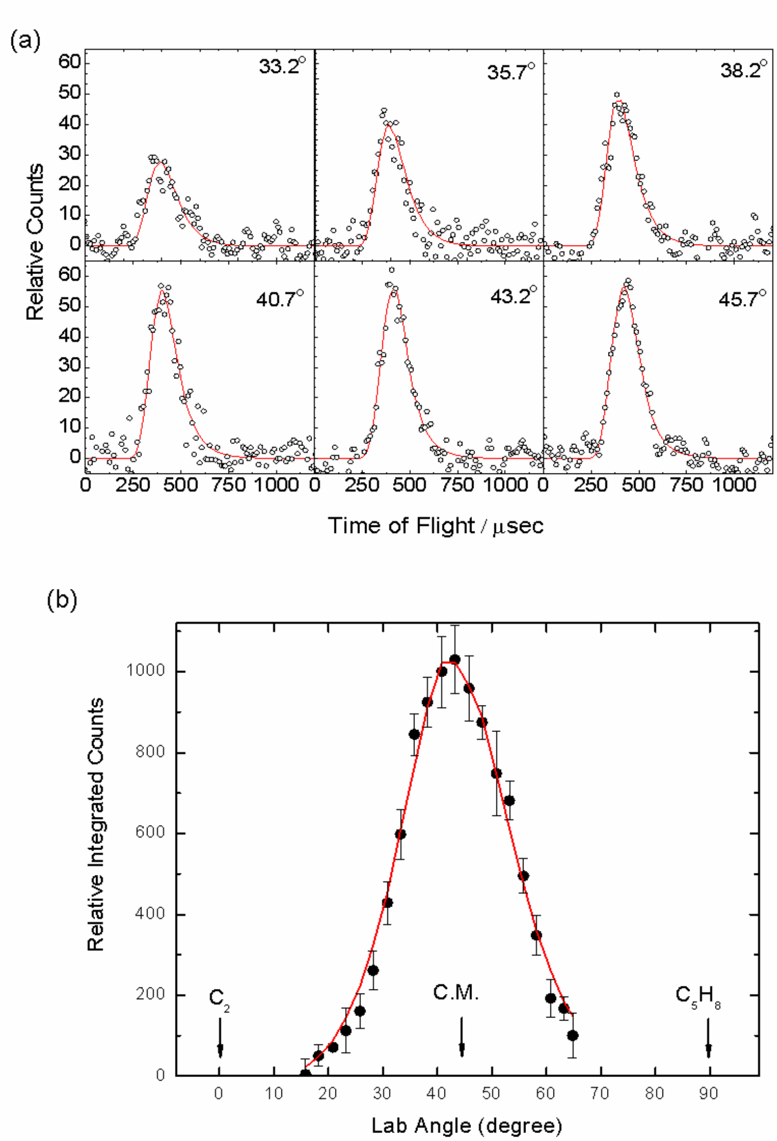
(a)
33.2°
35.7°
38.2°
40.7°
43.2°
45.7°
Relative Counts
Time of Flight / μsec
(b)
Relative Integrated Counts
Lab Angle (degree)
C₂
C.M.
C₅H₈

Figure 1

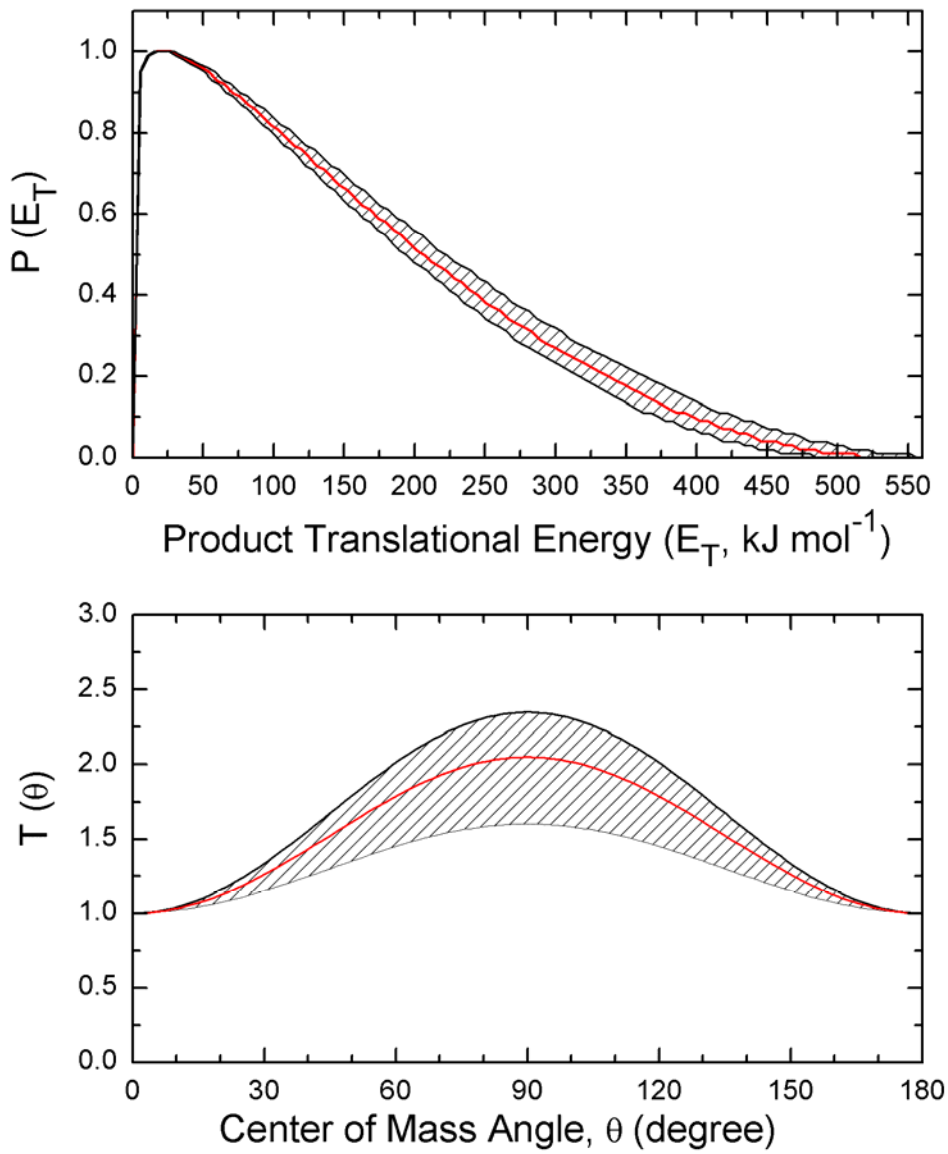
P (E_T)
1.0
0.8
0.6
0.4
0.2
0.0
0
50
100
150
200
250
300
350
400
450
500
550
Product Translational Energy (E_T, kJ mol^-1)
T (θ)
3.0
2.5
2.0
1.5
1.0
0.5
0.0
0
30
60
90
120
150
180
Center of Mass Angle, θ (degree)

Figure 2

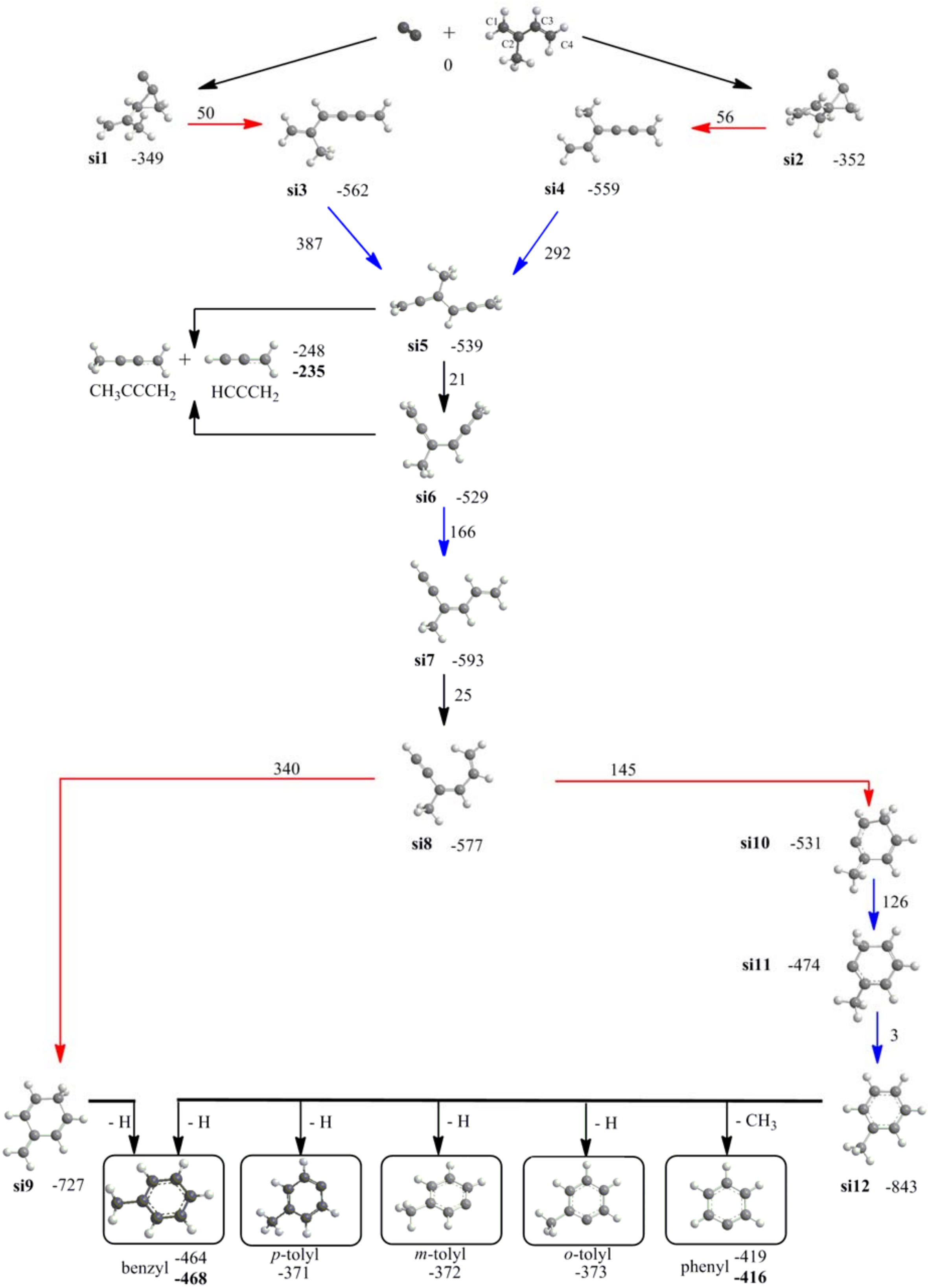

C1
C2
C3
C4
0
50
56
si1 -349
si2 -352
si3 -562
si4 -559
387
292
si5 -539
-248
-235
CH3CCCH2
HCCCH2
21
si6 -529
166
si7 -593
25
340
145
si8 -577
si10 -531
126
si11 -474
3
si9 -727
si12 -843
- H
- H
- H
- H
- H
- CH3
benzyl -464
-468
p-tolyl
-371
m-tolyl
-372
o-tolyl
-373
phenyl -419
-416

Figure 3

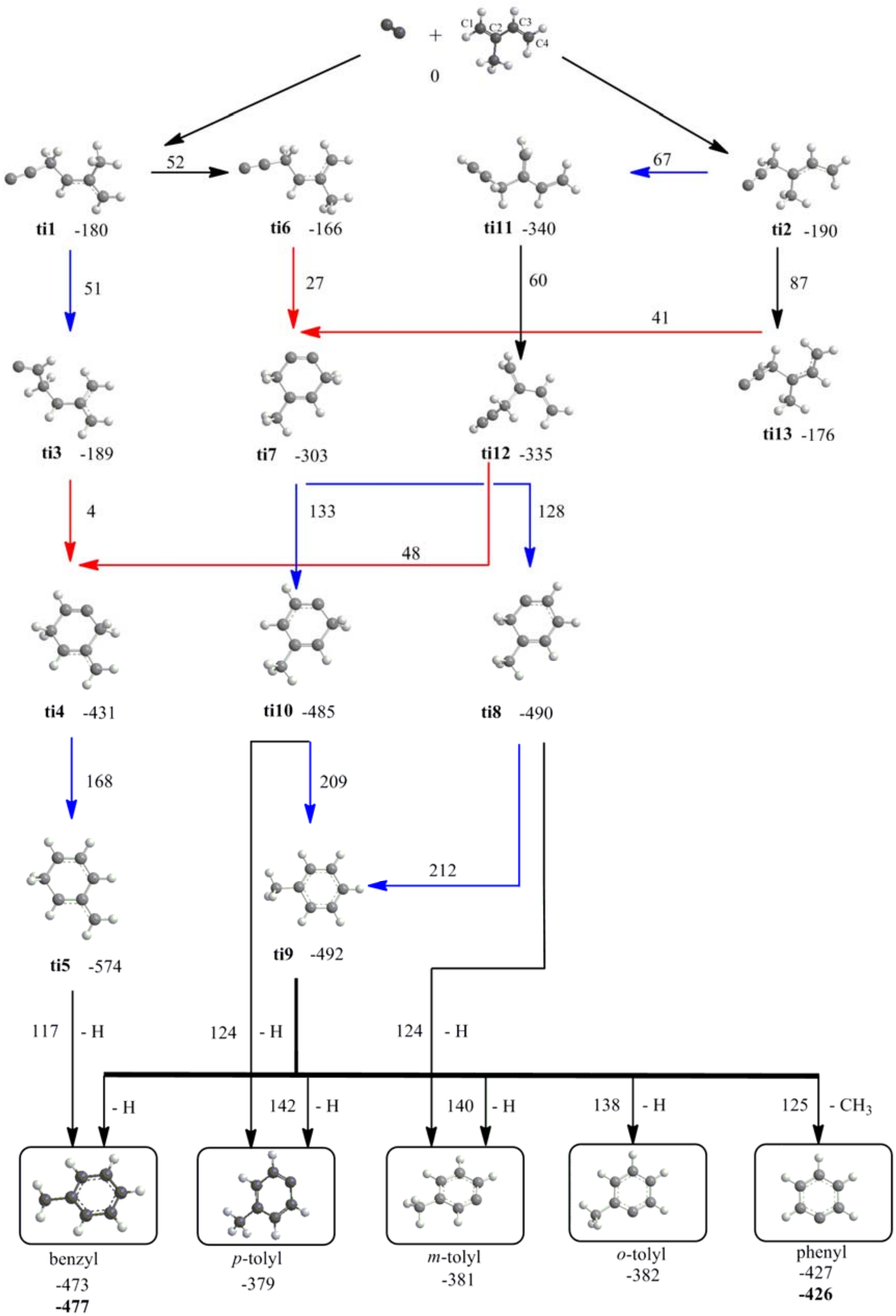
+
C1
C2
C3
C4
0
52
67
ti1 -180
ti6 -166
ti11 -340
ti2 -190
51
27
60
87
41
ti3 -189
ti7 -303
ti12 -335
ti13 -176
4
133
128
48
ti4 -431
ti10 -485
ti8 -490
168
209
212
ti5 -574
ti9 -492
117
- H
124
- H
124
- H
- H
142
- H
140
- H
138
- H
125
- CH3
benzyl
-473
-477
p-tolyl
-379
m-tolyl
-381
o-tolyl
-382
phenyl
-427
-426

Figure 4

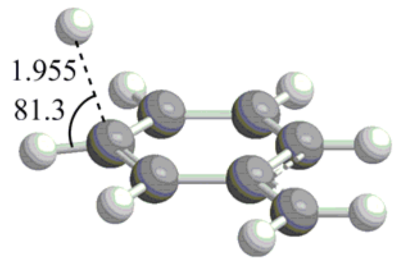

Figure 5

Supporting information for anie.201310612

Materials and Methods

Experimental: The experiments were conducted under single collision conditions utilizing a universal crossed molecular beam machine.[1] The dicarbon beam, $C_2(X^1\Sigma_g^+, a^3\Pi_u)$, was generated via laser ablation of graphite by seeding the ablation species in helium gas. The molecular beam passed a skimmer and a four-slot chopper wheel, which selected a segment of the pulsed dicarbon beam with a well-defined peak velocity of 2077±50 ms^{-1} and speed ratio 2.0±0.4. The segment of the pulsed dicarbon beam then crossed a pulsed 2-methyl-1,3-butadiene beam perpendicularly in the interaction region. The 2-methyl-1,3-butadiene peak velocity of 720±10 ms^{-1} and speed ratio 8.3±0.2 results in a collision energy of 42.7±1.5 kJ mol^{-1} and center-of-mass angle 44.1 ± 1.3^0. The neutral reaction products were analyzed by a triply differentially pumped rotatable mass spectrometer operated in time-of-flight (TOF) mode and ionized by electron impact at 80 eV, which then passed through a quadrupole mass filter and reached a Daly type ion detector. The TOF spectra were recorded at multiple angles and then integrated to obtain the angular distribution of the product(s). A forward-convolution routine[2] was used to fit the experimental data. The ro-vibrational distributions of the singlet $(X^1\Sigma_g^+)$ and triplet $(a^3\Pi_u)$ electronic states of the dicarbon beam were characterized spectroscopically *in situ* via laser induced fluorescence (LIF).[1]

Theoretical : Stationary points on the singlet and triplet C_7H_8 PES accessed by the reaction of dicarbon, $C_2(X^1\Sigma_g^+/a^3\Pi_u)$, with 2-methyl-1,3-butadiene, including intermediates, transition states, and possible products, were optimized at the hybrid density functional B3LYP level of theory with the 6-311G** basis set. Vibrational frequencies were computed using the same B3LYP/6-311G** method and were used to obtain zero-point vibrational energy (ZPE) corrections. Relative energies of various species were refined employing the coupled cluster CCSD(T) method with Dunning's correlation-consistent cc-pVDZ and cc-pVTZ basis sets. The total energies were extrapolated to the complete basis set (CBS) limit using the equation $E_{total}(CBS) = (E_{total}(VTZ)-E_{total}(VDZ)\times2.5^3/3.5^3)/(1-2.5^3/3.5^3)$.[3] For selected reaction products, we carried out CCSD(T)/cc-pVQZ calculations and extrapolated CCSD(T)/CBS total energies using the following formula, $E_{tot}(x) = E_{tot}(\infty) + Be^{-Cx}$, where x is the cardinal number of the basis set (2, 3, and 4) and $E_{tot}(\infty)$ is the CCSD(T)/CBS total energy.[4] Relative energies discussed in the paper are thus computed at the CCSD(T)/CBS//B3LYP/6-311G** + ZPE(B3LYP/6-311G**) level of theory with two-point (dt) and three-point (dtq) CBS extrapolations and are expected to be accurate within $\underline{+}15$ and $\underline{+}10$ kJ mol^{-1}, respectively. The B3LYP and CCSD(T) quantum chemical calculations were performed using the GAUSSIAN 09[5] and MOLPRO 2010[6] program packages. Unimolecular rate constants were computed using Rice-Ramsperger-Kassel-Marcus (RRKM) theory,[7] the rate constants were then utilized to calculate product branching ratios by solving first-order kinetic equations within steady-state approximation.

[1] R. I. Kaiser, P. Maksyutenko, C. Ennis, F. T. Zhang, X. B. Gu, S. P. Krishtal, A. M. Mebel, O. Kostko, M. Ahmed, *Faraday Discuss.* **2010**, *147*, 429.

[2] M. Vernon, Ph. D. thesis, University of California, Berkeley (Berkeley, CA), **1981**.

[3] S. B. Huh, J. S. Lee, *J. Chem. Phys.* **2003**, *118*, 3035.

[4] K. A. Peterson, T. H. Dunning, *J. Phys. Chem.* **1995**, *99*, 3898.

[5] M. J. Frisch, et al., Gaussian, Inc, Wallingford CT, **2009**.

[6] H.-J. Werner, P. J. Knowles, G. Kinizia, F. R. Manby, M. Schutz, P. Celani, T. Korona, R. Lindh, 2010 ed., **2010**, p. http://molpro.net.

[7] J. I. Steinfeld, J. S. Francisco, W. L. Hase, *Chemical Kinetics and Dynamics*, 2nd ed., Prentice Hall, New Jersey, **1999**.

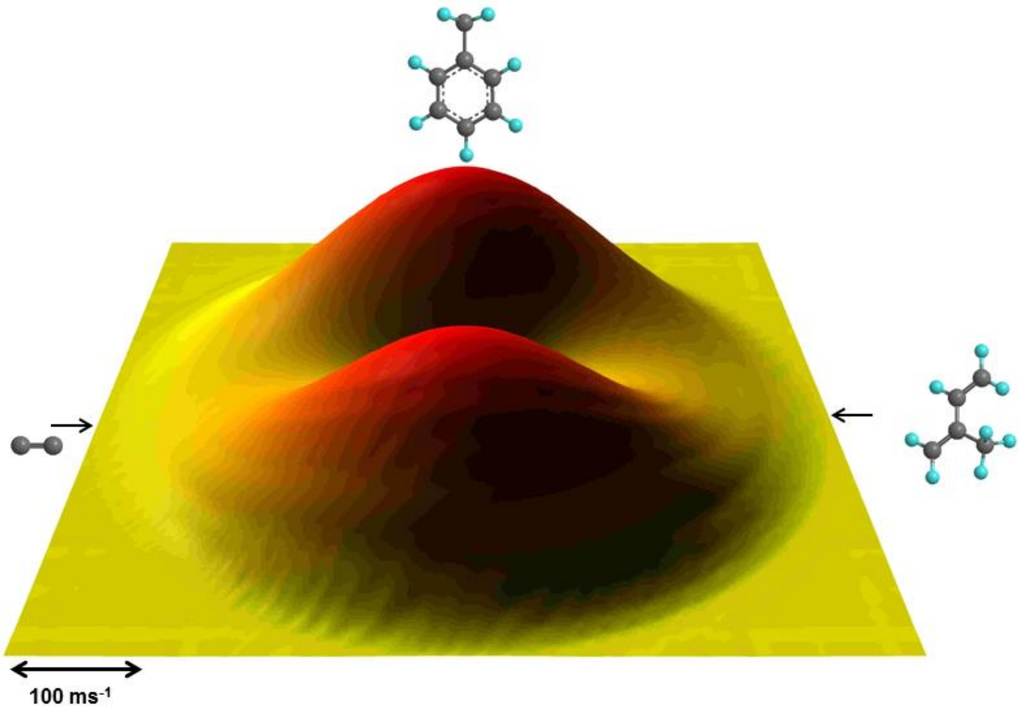

Figure: TOC

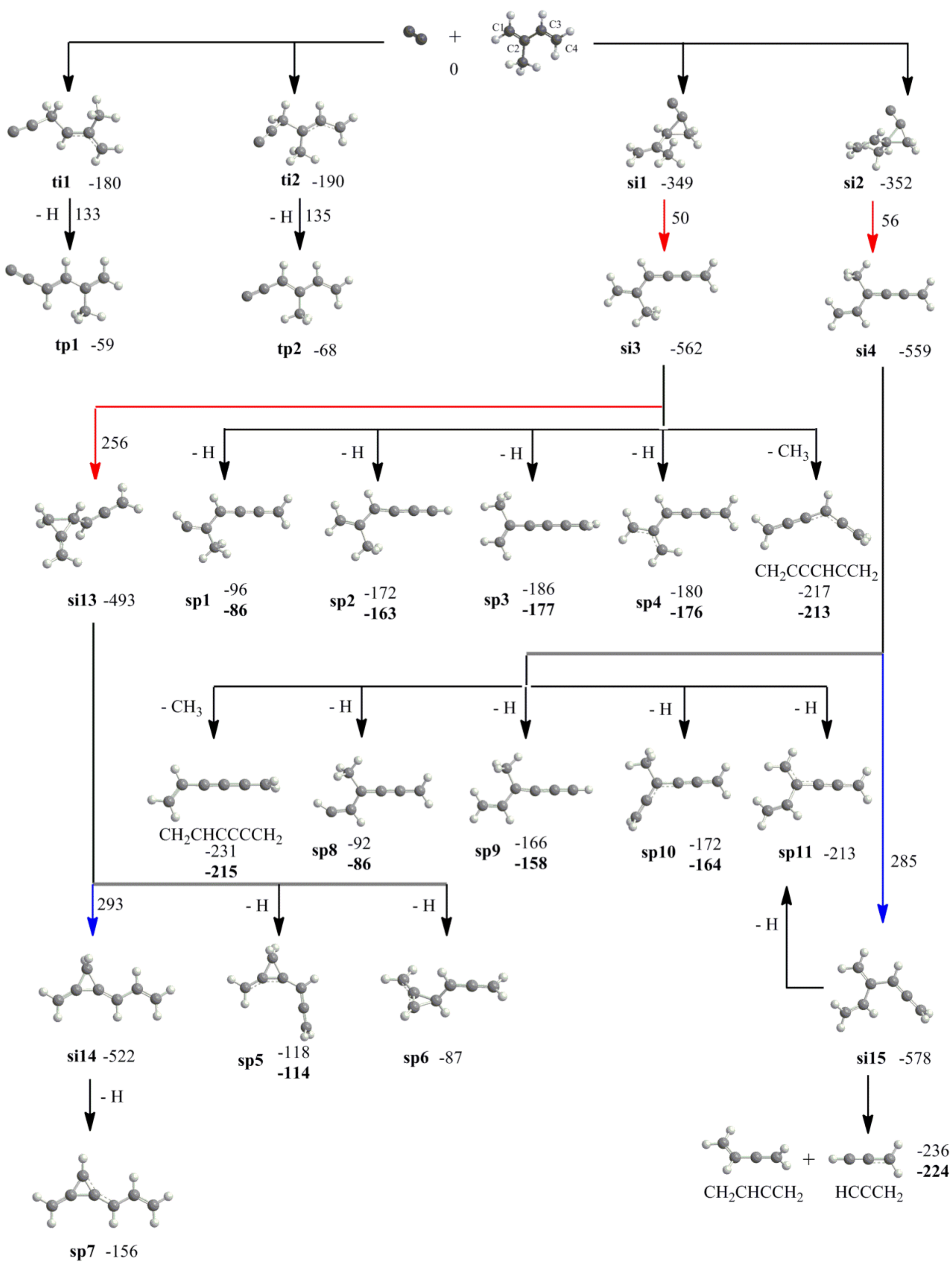

Figure S1: Reaction paths leading to the acyclic or tricyclic products in the dicarbon isoprene reaction. **t**, **s**, **i** and **p** represent the triplet, singlet, intermediate and product, respectively. Corresponding total energies with respect to the reactants and barrier heights (where applicable) are also shown in the units of kJ mol^{-1} as calculated at the CCSD(T)/CBS(dt)//B3LYP/6-311G** + ZPE(B3LYP/6-311G**) (plain numbers) and CCSD(T)/CBS(dtq)//B3LYP/6-311G** + ZPE(B3LYP/6-311G**) (bold numbers) levels of theory. Hydrogen shifts and isomerization via ring closure/opening are presented via blue and red arrows, respectively. For clarification, the carbon atoms in isoprene are labeled as C1 to C4.